J. of the Braz. Soc. Mechanical Sciences, Vol. XXIII, No 3, pp.253-267, 2001

Chaos and Unpredictability in the Vibration of an Elasto-Plastic Beam

Marcelo A. Savi
Department of Mechanical and Materials Engineering
Instituto Militar de Engenharia
22.290.270 Rio de Janeiro, RJ. Brazil
savi@ime.eb.br
Pedro M. C. L. Pacheco
Department of Mechanical Engineering, CEFET/RJ
20.271.110 Rio de Janeiro, RJ. Brazil
calas@cefet-rj.br

This contribution discusses the nonlinear dynamics of a pin-ended elasto-plastic beam with both kinematic and isotropic hardening. An iterative numerical procedure based on the operator split technique is developed in order to deal with the nonlinearities in the equations of motion. Free and forced responses for harmonic sinusoidal and square wave excitations are investigated. Numerical simulations present many interesting behaviors such as jump phenomena, sensitivity to initial conditions, chaos and transient chaos. These results indicate that there are practical problems in predicting the response of the beam even when periodic steady state response is expected.
Keywords*: Chaos, Nonlinear Dynamics, Elasto-plasticity, Beam Vibration.*

Introduction

The study of elasto-plastic structures is important in many engineering problems and the dynamical response of these systems is very rich. Shanley (1947) proposes a model where a pin-ended beam is represented by two rigid links joined by an elasto-plastic element, referred as a cell. This element has two short flanges where each one is elastic-perfectly plastic and therefore, hardening effect is not considered. Symonds and Yu (1985) studied this problem either by finite element method or by employing a simplified Shanley model. Poddar *et al.* (1988) investigate the chaotic behavior of the Symonds' model when it is periodically excited by a series of positive and negative impulses. Many other studies are focused on the response of different elasto-plastic oscillators with bilinear hysteretic models. Pratap *et al.* (1994a,b) present a model where the elasto-plastic cell is replaced by a torsional spring and kinematic hardening is considered to describe the constitutive behavior of this spring. Judge and Pratap (1998) revisit this problem including viscous damping in the analysis. Savi and Pacheco (1997) consider an elasto-plastic oscillator with both kinematic and isotropic hardening, proposing a numerical procedure to solve equations of motion. Chaotic motion is also concerned in the studies of Pratap and Holmes (1995) and Symonds *et al.* (1986).

The present work revisits the Symonds' model. Small displacement hypothesis, considered on the earlier models, is not assumed here. Ideal plasticity and hardening effect are both in focus. The hardening effect is represented by a combination of kinematic and isotropic hardening and the inclusion of these effects on the Symonds' model represents one of the main contributions of this article. The operator split technique (Ortiz *et al.*, 1983) associated with an iterative numerical procedure is developed in order to deal with the nonlinearities in the equations of motion. As in Savi and Pacheco (1997), which uses a similar algorithm, the proposed procedure proved to be an efficient tool to simulate nonlinear dynamical systems. In order to show the potentiality of the proposed algorithm, two different excitations are conceived: harmonic sinusoidal and square wave. Numerical investigations for free and forced responses present many interesting behaviors such as jump phenomena, sensitivity to initial conditions, chaos and transient chaos.

Model for an Elasto-Plastic Beam

Shanley (1947) proposes a model where a pin-ended beam with length $2L$, and uniform rectangular cross section of area $A = ba'$, is represented by two rigid links, each of length L, joined by an elasto-plastic element. The two rigid bars are assumed to have mass per unit length ρ, the same as for the uniform beam. The beam model is depicted in Figure 1.

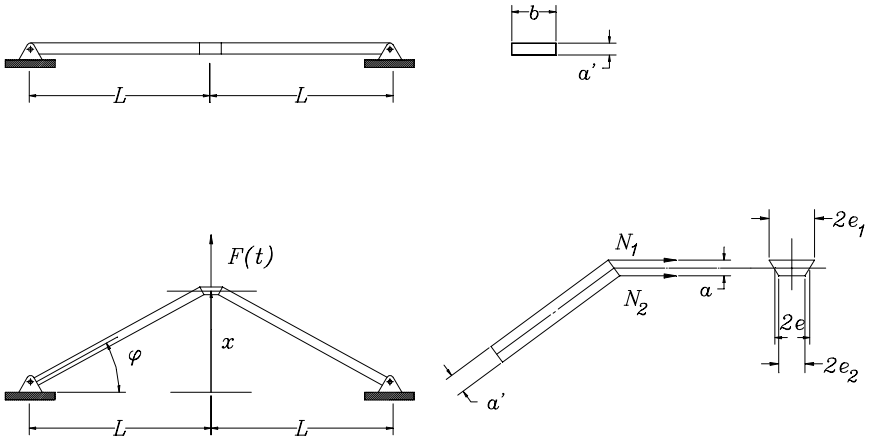

Figure 1. Elasto-plastic beam.

Geometric considerations allows one to define the relation between the cell position, x, and the angle of rotation, φ. Also, it is possible to establish similar relations involving the semi-extension of the cell centerline, e, and the semi-extension of each flange, e_1 and e_2, as follows

$$x = L\sin\varphi$$

$$e = L(\cos\varphi_0 - \cos\varphi)\ ,\quad e_1 = e + \frac{a}{2}\sin\varphi\quad ,\quad e_2 = e - \frac{a}{2}\sin\varphi\ . \tag{1}$$

where φ_0 defines the angle φ at the initial instant.

In the present article, a constitutive equation with linear kinematic and isotropic hardening is considered (Savi and Pacheco, 1997),

$$\sigma = E(\varepsilon - \varepsilon^p)\ ,$$

$$\dot{\varepsilon}^p = \gamma\,\mathrm{sign}(\sigma - \beta)\ ,\ \dot{\alpha} = \gamma\ ,\quad \dot{\beta} = \gamma H\,\mathrm{sign}(\sigma - \beta)\,, \tag{2}$$

where sign(•) = (•) / | • |; σ is the one-dimensional stress, ε and ε^p are the total and plastic one-dimensional strain, respectively; β is the back stress and α is the internal hardening variable. The variables β and α are associated with kinematic and isotropic hardening, respectively, and γ represents the rate at which plastic deformations take place. The parameter E is the Young modulus and H is the kinematic hardening parameter.

The yield function, $h(\sigma,\alpha,\beta)$, the Kuhn-Tucker conditions and the consistency condition are given by (Savi and Pacheco, 1997):

$$h(\sigma,\alpha,\beta) = |\sigma - \beta| - (\sigma_Y + K\alpha)$$

$$\gamma \geq 0\ ,\quad \gamma h(\sigma,\alpha,\beta) = 0\ ,\quad \gamma \dot{h}(\sigma,\alpha,\beta) = 0 \quad \text{if} \quad h(\sigma,\alpha,\beta) = 0\ . \tag{3}$$

Here, K is the plastic modulus and σ_Y is the yield stress. The yield function shows that kinematic hardening causes the elastic domain translation, while isotropic hardening causes its expansion.

The force and moment resultants in the cell (N and M, respectively) are taken by considering the same relations of those of a sandwich beam, consisting of two bars each in simple tension or

compression (Symonds and Yu, 1985). Hence, employing indices 1 and 2 to denote the variables on each flange,

$$N = N_1 + N_2 = \int_A \sigma_1 dA + \int_A \sigma_2 dA \tag{4}$$

$$M = (N_2 - N_1)\frac{a}{2} \tag{5}$$

where A is the area on each flange.

Assuming that the total strain on each flange is obtained by dividing the semi-extension by the semi-length of the beam, and the area of each flange is a half of the beam cross section area, the following relation is written

$$N_i = \frac{EA}{2L}(e_i - e_i^p) \quad (i = 1,2) \tag{6}$$

where e_i^p is the plastic semi-extension on each flange.

In order to formulate the governing equations of the model, equilibrium of moment on the half beam are established. Neglecting the inertia of the elasto-plastic element and assuming a linear viscous external dissipation,

$$\ddot{\varphi} + \mu c\,\dot{\varphi} + \mu L\, N \sin\varphi - \mu M = \frac{\mu L}{2} F(t) \tag{7}$$

where $\mu = 3 / \rho L^3$ and c is the linear viscous dissipation parameter. N and M are given by equations (1-6). Now, consider the following definitions,

$$\omega_0^2 = \mu L\, N_y \ , \ c_0 = \mu c / \omega_0 \ , \ \mu_0 = M_y / L\, N_y \ , \ f = F / 2N_Y \ , \ \tau = \omega_0 t$$
$$n = N / N_Y \ , \ m = M / M_Y \tag{8}$$

where $N_Y = \sigma_Y A$ and $M_Y = N_Y\, a/2$. Denoting the non-dimensional time derivative by $(\,)' = d(\,)/d\tau$, the following system can be written,

$$\begin{aligned} y_1' &= y_2 \\ y_2' &= -c_0 y_2 - n \sin y_1 + \mu_0 m + f(\tau) \end{aligned} \tag{9}$$

As a matter of fact, the state space includes more variables than y_1 and y_2 (Poddar *et al.*, 1988), however, the analysis is developed on a subspace of dimension 2 (Savi and Pacheco, 1997). The numerical solution procedure here proposed uses the operator split technique (Ortiz *et al.*, 1983), associated with an iterative procedure in order to assure the convergence of the process (Savi and Pacheco, 1997). In the first step of the procedure, equation (9) is integrated employing any classical scheme, like fourth order Runge-Kutta, assuming that variables n and m are known parameters which are evaluated with an elastic predictor step, where plastic variable, ε^p, remains constant from the previous time instant. The next step of solution procedure consists on a plastic corrector step where the feasibility of the trial state is evaluated employing the return mapping algorithm (Simo and Taylor, 1985). In order to assure the convergence of the process, these steps must be repeated until the values converge for two consecutive iterations.

Free Vibrations

In this Section, the free response of the elasto-plastic beam is discussed. This is done by letting $f(\tau)$ vanish in the equations of motion (9). Free response of the elasto-perfectly plastic beam and the hardening beam are similar. In all simulations, one has taken L = 0.10m, b = 0.02m, a' = 0.04m, a = 0.68a', ρ = 0.216 kg/m, E = 120 GPa, σ_Y = 0.3 GPa, K = 0.10 GPa, H = 0.44 GPa (Poddar *et al.*, 1988). Also, the initial condition φ_0 = 0 is considered. The procedure converges with time steps with 1,000 points per period.

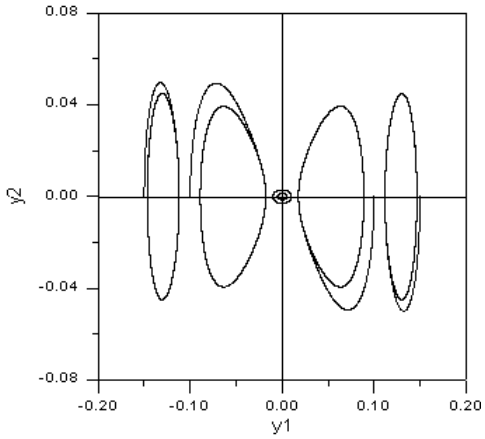

Figure 2. Phase portrait.

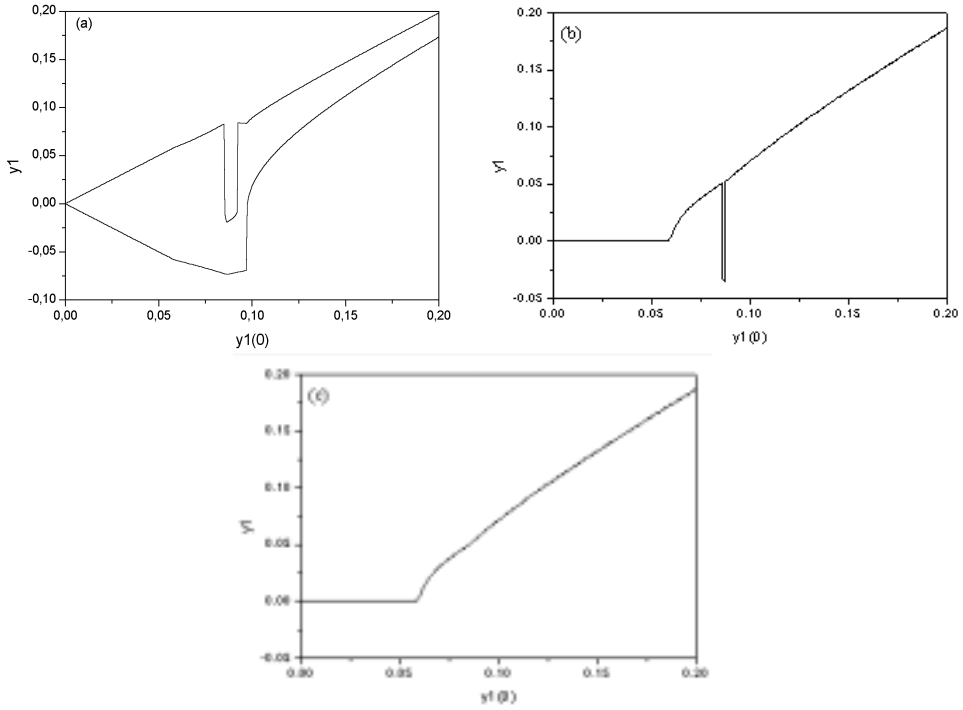

Figure 3. Steady state envelope of maximum and minimum angular displacement for different initial conditions. (a) c_0 = 0; (b) c_0 = 0.2; (c) c_0 = 1.5.

In order to illustrate the free response, a system with no external dissipation is considered ($c_0 = 0$). Figure 2 presents results from simulations in the form of phase portrait. Different initial conditions cause different plastification of the cell and, as a consequence, alter the position of equilibrium points in phase space.

Poddar *et al.* (1988) show the fractal basin boundaries of the system under free vibration, using this conclusion to explain the discrepancy among some finite element results shown in Symonds and Yu (1985). Figure 3 shows the steady state envelope of maximum and minimum angular displacement, y_1, for different initial conditions with null initial angular velocity. Figure 3a shows the response of a beam with no external dissipation ($c_0 = 0$), and reproduces the result obtained in Symonds and Yu (1985). Notice that a global change in the response occurs when initial conditions are in the range from 0.086 to 0.092. When an external dissipation is considered, asymptotic behavior is expected. Therefore, envelope of maximum and minimum angular displacement becomes a line. When $c_0 = 0.2$, global changes are characterized by jumps (Figure 3b). For high values of this parameter, for example $c_0 = 1.5$, global changes do not occur anymore (Figure 3c).

Ideal Plasticity

This section considers the forced response of the elastic-perfectly plastic beam. The constitutive equation for ideal plasticity theory may be obtained simplifying equations (2-3) as follows,

$$\sigma = E(\varepsilon - \varepsilon^p) \ , \quad \dot{\varepsilon}^p = \gamma \, \mathrm{sign}(\sigma) \tag{10}$$

The yield function, $h(\sigma)$, Kuhn-Tucker conditions and the consistency condition are now given by:

$$h(\sigma) = |\sigma| - \sigma_Y$$
$$\gamma \geq 0 \ , \ \gamma h(\sigma) = 0 \ , \ \gamma \dot{h}(\sigma) = 0 \quad \text{if} \quad h(\sigma) = 0 \ . \tag{11}$$

In order to analyze the forced response of elastic-perfectly plastic beam, the following sections discuss two different excitations: harmonic sinusoidal and square wave.

Harmonic Excitation

This section considers a beam subjected to a harmonic sinusoidal excitation, $f(\tau) = \delta \sin(\Omega\tau)$. Numerical simulations employs time steps smaller than $\Delta\tau = 2\pi / 1000\Omega$. In order to start the analysis, bifurcation diagrams representing the stroboscopically sampled angular displacement values, y_1, under the slow quasi-static increase of the driving force amplitude, δ, are considered. Dissipation parameter is $c_0 = 1.5$ and different values of frequency parameters are considered. The first 30 cycles are neglected (Figure 4).

These diagrams allow one to identify regions where a small variation in forcing amplitude causes a jump in the angular displacement value. The cloud of points, usually associated with chaotic motion, does not appear in the considered range of parameters.

In order to analyze jump phenomenon, steady state response is regarded. For frequency parameter $\Omega = 0.75$, jump occurs near $\delta = 0.17$ and again near $\delta = 0.30$. When $\Omega = 1$, the jump occurs for $\delta = 0.24$ and $\delta = 0.40$. Figure 5a shows steady state response for $\Omega = 0.75$ and two different driving force amplitudes very close: $\delta = 0.17$ and $\delta = 0.18$. Figure 5b shows similar behavior when frequency parameter is $\Omega = 1$ and driving force amplitudes are $\delta = 0.24$ and $\delta = 0.25$. Notice that small change in the forcing amplitude leads to a shift in the center of the steady state oscillations.

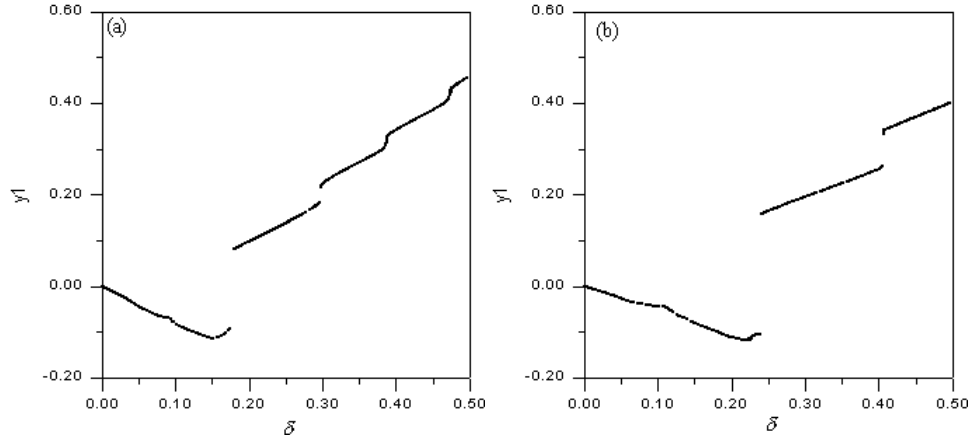

Figure 4. Bifurcation diagrams: Ideal plasticity and sinusoidal excitation. (a) $\Omega = 0.75$; (b) $\Omega = 1$.

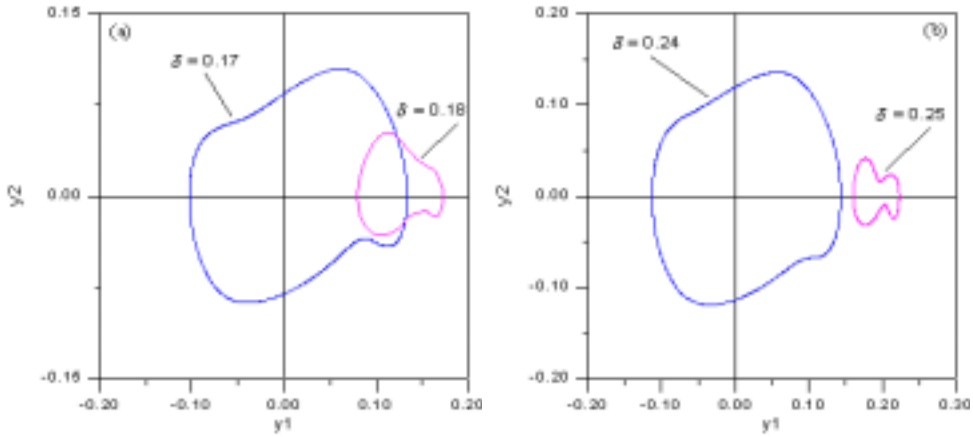

Figure 5. Jump phenomenon on the elasto-perfectly plastic beam subjected to sinusoidal excitation. (a) $\Omega = 0.75$, $\delta = 0.17$ and $\delta = 0.18$; (b) $\Omega = 1$, $\delta = 0.24$ and $\delta = 0.25$.

In spite of the beam does not exhibit chaotic motion with the previous physical parameters, jump phenomenon introduces difficulties to predict the beam behavior. Sensitivity to initial conditions also introduces this kind of difficulty. Poddar *et al.* (1988) show that chaotic motion occurs in Symonds' beam when it is subjected to periodic impulses. Therefore, it is interesting to consider different values of parameters to evaluate the possibility of chaotic motion. With this aim, a dissipation parameter c_0 = 0.2 is assumed. Figure 6 shows the bifurcation diagram with frequency parameter Ω = 1 and now, it is possible to identify regions with cloud of points associated with chaos.

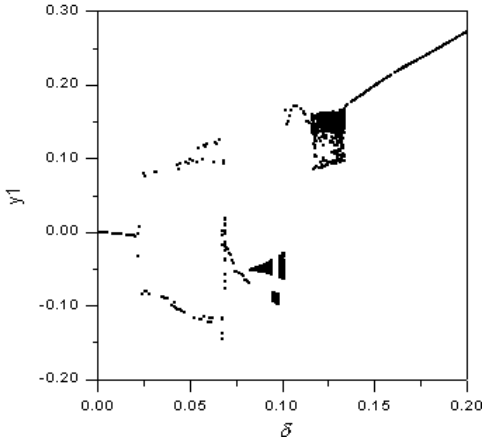

Figure 6. Bifurcation diagram: Ideal plasticity and sinusoidal excitation with c_0 = 0.2 and Ω = 1.

Figure 7a shows the strange attractor of the motion for δ = 0.13, while Figure 7b presents the periodic phase plane for δ = 0.15. The Fast Fourier Transform (FFT) analysis allows one to clearly identify the difference between both responses (Figure 8). As it is well known, the FFT of a chaotic signal presents continuous spectrum over a limited range. The energy is spread over a wider bandwidth. On the other hand, the FFT of a periodic signal presents discrete spectrum, where a finite number of frequencies contribute to the response (Moon, 1992; Mullin, 1993).

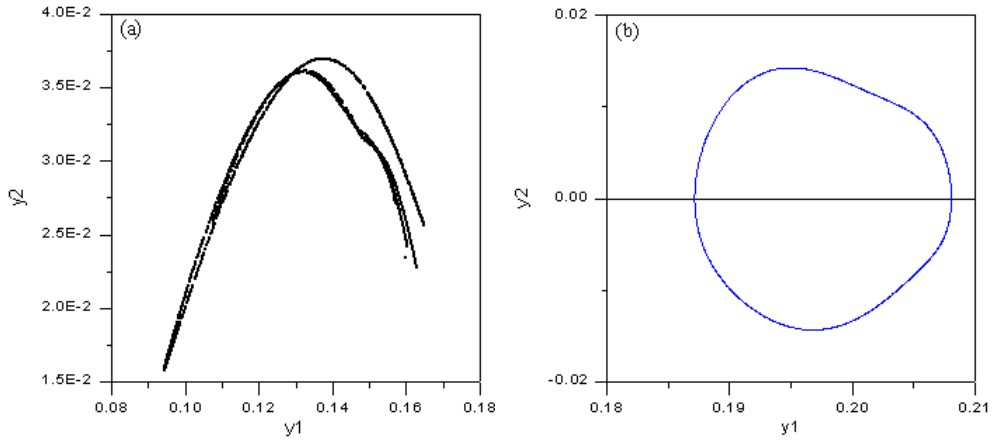

Figure 7. Response of the elasto-perfectly plastic beam subjected to sinusoidal excitation with Ω = 1 and c_0 = 0.2. (a) Strange attractor for δ = 0.13; (b) Phase plane for δ = 0.15.

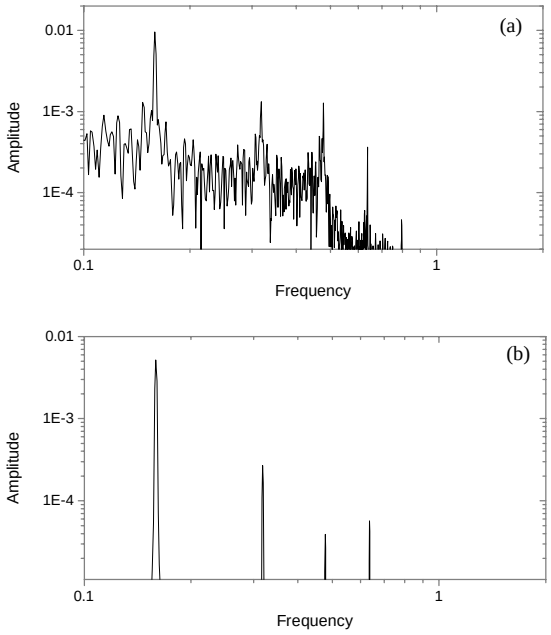

Figure 8. FFT analysis of the elasto-perfectly plastic beam subjected to sinusoidal excitation with $\Omega = 1$ and $c_0 = 0.2$. (a) Chaotic, $\delta = 0.13$; (b) Periodic, $\delta = 0.15$.

Square Wave Excitation

This section considers a beam subjected to a square wave excitation. As a matter of fact, the square wave uses 1% of the period to load or unload. In order to start the analysis, bifurcation diagrams are considered (Figure 9). Dissipation parameter is c_0 = 1.5 and different values of frequency parameters are conceived, neglecting the first 30 cycles.

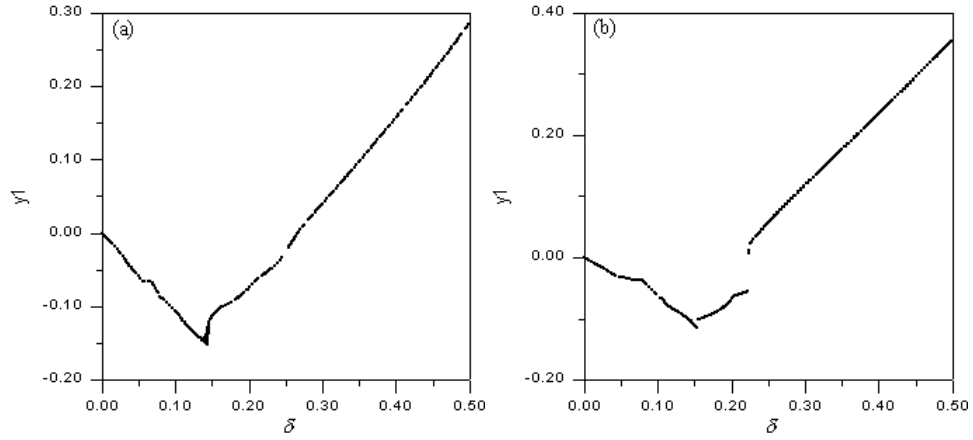

Figure 9. Bifurcation diagrams: Ideal plasticity and square wave excitation. (a) $\Omega = 0.75$; (b) $\Omega = 1$.

The response of the beam subjected to square wave excitation is similar to the response obtained under harmonic excitation. Observing bifurcation diagrams it is possible to see jump phenomenon for different driving force amplitude. As in the previous section, notice that even when a periodic elasto-plastic response is expected, jump phenomenon introduces difficulties to predict the beam behavior.

Chaotic motion may also occur when parameter dissipation is altered for c_0 = 0.2, for example. Figure 10 shows the bifurcation diagram for this situation when Ω = 1. The strange attractor of the motion for δ = 0.08 is depicted in Figure 11a, while Figure 11b presents the periodic phase plane for δ = 0.04.

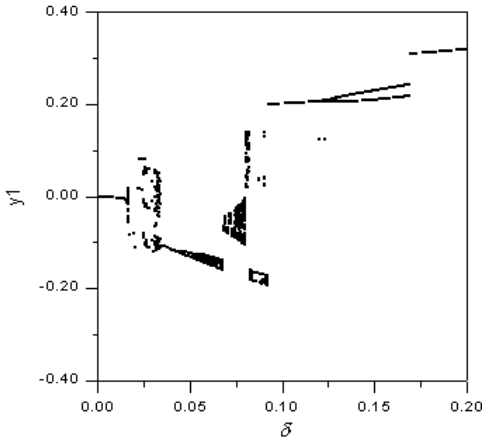

Figure 10. Bifurcation diagram: Ideal plasticity and square wave excitation with c_0 = 0.2 and Ω = 1.

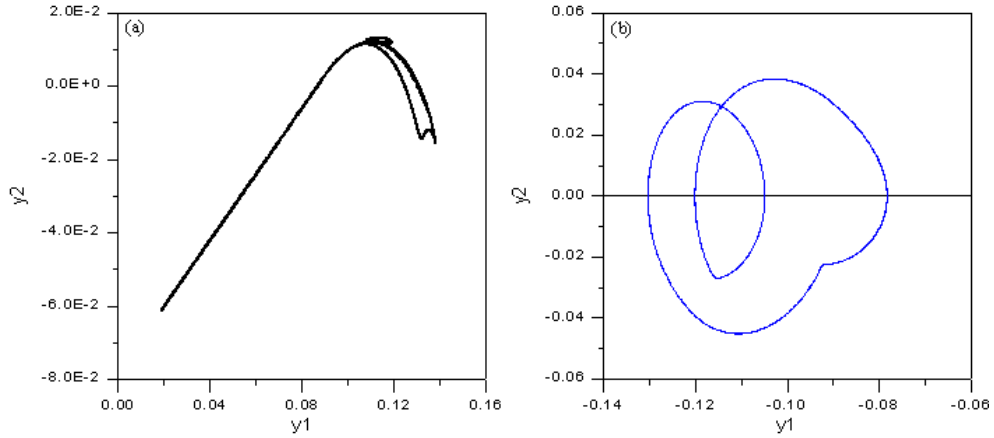

Figure 11. Response of the elasto-perfectly plastic beam subjected to square wave excitation with Ω = 1 and c_0 = 0.2. (a) Strange attractor for δ = 0.08; (b) Phase plane for δ = 0.04.

Kinematic and Isotropic Hardening

At this time, the forced response of the elasto-plastic beam with hardening is considered. Kinematic and isotropic hardening are both included in the model and the constitutive behavior is described by equations (2-3). Again, in order to analyze the forced response of hardening model beam, the following sections discuss two different excitations: harmonic sinusoidal and square wave.

Harmonic Excitation

This section presents the beam response under harmonic sinusoidal excitation, $f(\tau) = \delta \sin(\Omega\tau)$. Numerical simulations considers time steps smaller than $\Delta\tau = 2\pi / 1000\Omega$. Savi and Pacheco (1997) show that an elasto-plastic oscillator with isotropic hardening tends to an elastic steady state response. For the same reasons, similar behavior may be expected in the beam response and, therefore, after a transient, an elastic steady state is reached where plastic variables remain constant.

Once again, the analysis begins considering bifurcation diagrams which presents stroboscopically sampled angular displacement values, y_1, under the slow quasi-static increase of the driving force amplitude, δ. The dissipation parameter is $c_0 = 1.5$ and different values of frequency parameters are considered. Only the first 30 cycles are neglected, even though the steady state response is not reached. These bifurcation diagrams show regions with clouds of points, usually associated to chaotic behavior, and jumps (Figure 12).

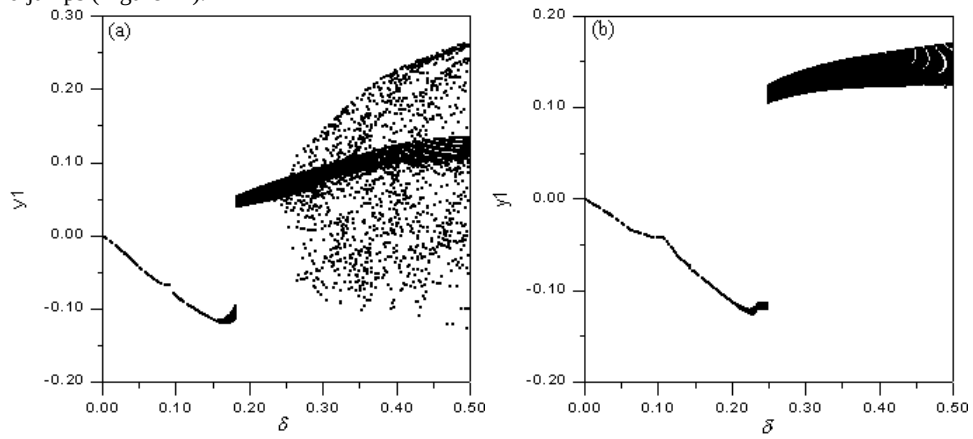

Figure 12. Bifurcation diagrams: Hardening and sinusoidal excitation. (a) $\Omega = 0.75$; (b) $\Omega = 1$.

Figure 13 shows the Poincaré section of the motion when $\Omega = 0.75$ and $\delta = 0.3$, presenting a transient strange attractor. Notice that after 1300 cycles, this motion tends to a single point meaning a periodic response. The FFT analysis allows one to clearly identify the difference between the two kinds of response. During transient chaos, the FFT presents continuous spectrum (Figure 14a). After this transient, the response becomes periodic, and the FFT presents discrete spectrum (Figure 14b).

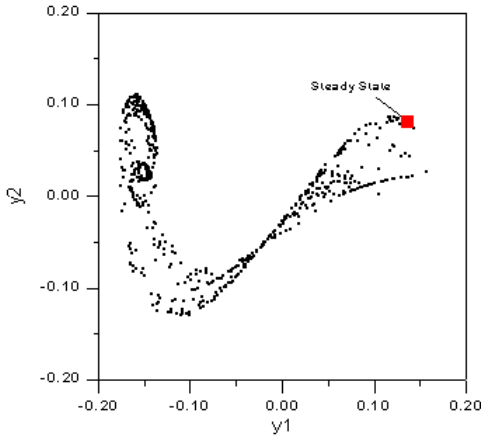

Figure 13. Transient strange attractor: Sinusoidal excitation ($\Omega = 0.75$, $\delta = 0.3$).

As it is well known, chaotic motion presents sensitivity to initial conditions and, in spite of the periodic steady state behavior, transient chaos causes unpredictability. Assuming different initial conditions, very close from the previous case, different steady state responses may be observed. Figure 15 illustrates this behavior. The previous example considers $(y_1, y_2) = (0,0)$, and other situations are analyzed for $(y_1, y_2) = (0,-1e-4)$, $(y_1, y_2) = (0,+1e-4)$, $(y_1, y_2) = (-2.5e-4,0)$ and $(y_1, y_2) = (+2.5e-4,0)$. These conditions represent variations less than 0.1% of the maximum angular displacement and velocity at steady state. Hence, transient chaos may cause practical problems in predicting the beam response.

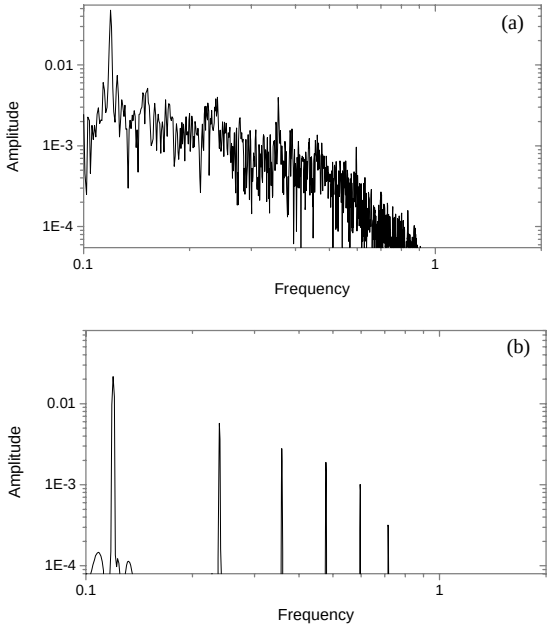

Figure 14. FFT analysis of the beam including hardening effect subjected to sinusoidal excitation with $\Omega = 0.75$, $\delta = 0.3$. (a) Transient chaos (500th to 632nd cycles); (b) Steady State (1300th to 1432nd cycles). (a) Transient chaos (500th to 632nd cycles); (b) Steady State (1300th to 1432nd cycles).

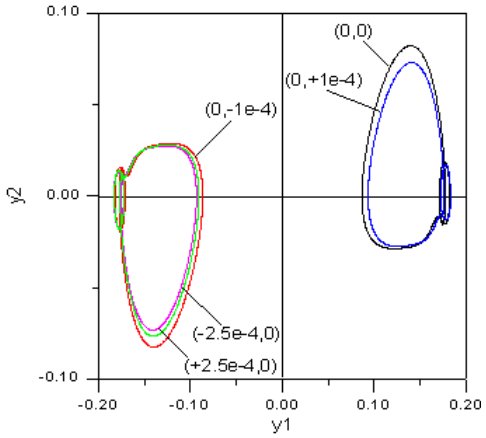

Figure 15. Steady state response of the beam including hardening effect subjected to sinusoidal excitation with $\Omega = 0.75$, $\delta = 0.3$. Different initial conditions are considered for (y_1, y_2): (0,0), (0,–1e–4), (0,+1e–4), (–2.5e–4,0) and (+2.5e–4,0).

Grebogi *et al.* (1983) defines crises phenomenon as a collision between a chaotic attractor and a coexisting unstable fixed point or periodic orbit. In this situation, chaotic behavior appears or disappears for some parameter change. In transient chaos, after a finite time, the orbit leaves the chaotic region, establishing a periodic or quasiperiodic motion (Moon, 1992). The term transient chaos is used here to describe a chaotic-like response, which becomes periodic after some cycles. A particular set of physical parameters is considered. This behavior may be understood as the crises of the system where the parameters are represented by the internal variables related to plastic behavior, with values varying in time.

As can be seen in bifurcation diagrams, jump phenomenon also exists on the response of the hardening beam. When $\Omega = 1$, jump is near $\delta = 0.25$. Figure 16 shows steady state response for $\Omega = 1$ and two forcing amplitudes very close ($\delta = 0.24$ and $\delta = 0.25$). Again, small change in the forcing amplitude leads to different positions of the steady state oscillations in phase space.

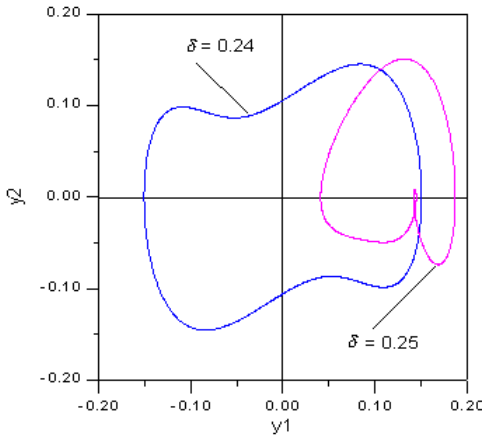

Figure 16. Jump phenomenon on the beam including hardening effect subjected to sinusoidal excitation with $\Omega = 1$ and two forcing amplitudes $\delta = 0.24$ and $\delta = 0.25$.

Square Wave Excitation

A square wave excitation is now in focus. Initially, bifurcation diagrams are considered where dissipation parameter is $c_0 = 1.5$ and different values of frequency parameters are considered. Only the first 30 cycles are neglected, even though the steady state response is not reached (Figure 17).

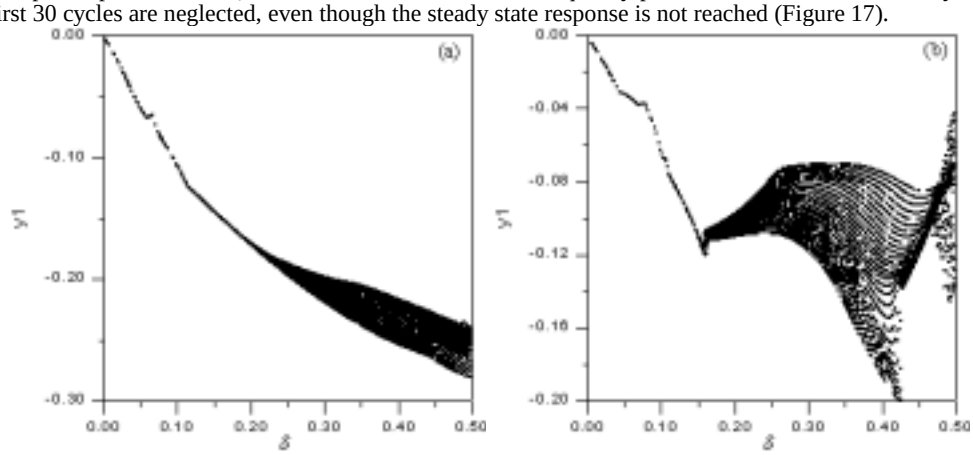

Figure 17. Bifurcation diagrams: Hardening and square wave excitation. (a) $\Omega = 0.75$; (b) $\Omega = 1$.

Transient chaos may also exist when the beam is subjected to a square wave excitation. In order to establish a comparison between the sinusoidal and square wave excitation, one conceives an example treated in the preceding section with $\Omega = 1$ and $\delta = 0.5$. In this example simulation, a transient strange attractor occurs during transient chaos and, after this, the response converges to a small region of the phase space (Figure 18).

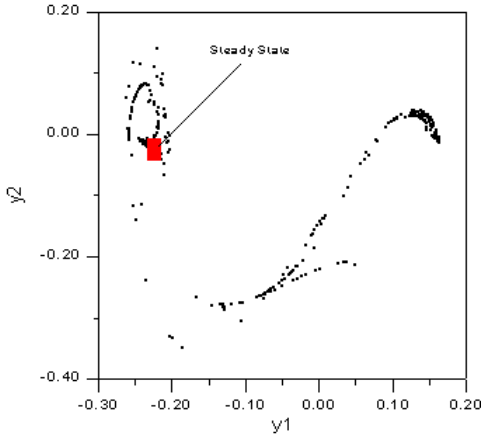

Figure 18. Transient strange attractor: Square wave excitation ($\Omega = 1$, $\delta = 0.5$).

Small variations on initial conditions may cause, again, considerable changes in the steady state response of the beam. In order to illustrate this, one investigates the same variations imposed on the previous section, that is, $(y_1, y_2) = (0,0)$, $(y_1, y_2) = (0,-1e-4)$, $(y_1, y_2) = (0,+1e-4)$, $(y_1, y_2) = (-2.5e-4,0)$ and $(y_1, y_2) = (+2.5e-4,0)$, which are presented in Figure 19.

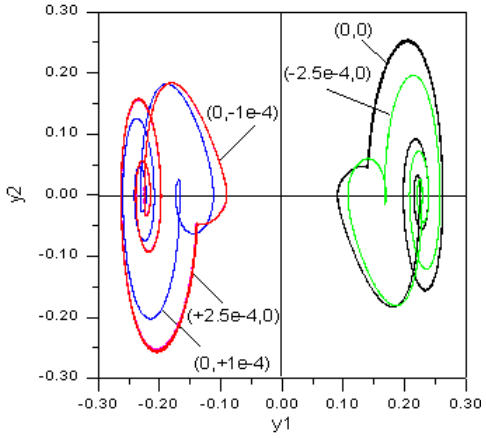

Figure 19. Steady state response of the beam including hardening effect subjected to square wave excitation with $\Omega = 1$, $\delta = 0.5$. Different initial conditions are considered for (y_1, y_2): (0,0), (0,–1e–4), (0,+1e–4), (–2.5e–4,0) and (+2.5e–4,0).

Conclusions

A dynamical analysis of the Symonds' model for a pin-ended elasto-plastic beam is considered. Ideal plasticity theory and hardening effect are both in focus. The numerical method proposed in this work proved to be an efficient tool to evaluate the response of elasto-plastic dynamical systems, and allows

the use of a combination of classical algorithms. Numerical simulations for forced vibrations subjected to harmonic sinusoidal and square wave excitation are evaluated. Results show that the beam response has many interesting behaviors. Jump phenomenon causes considerable variations in the steady state response for very small changes in the forcing parameter. Transient chaos, which may exists when the hardening effect is included in the model, may be understood as the crises of the system where the parameters are represented by the internal variables related to plastic behavior, with values varying in time. Sensitivity to initial conditions may occur as a consequence of fractal basin boundaries and/or transient chaos. All these effects may cause practical problems in predicting the response of the beam even when a periodic steady state response is expected.

Acknowledgements

The authors acknowledge the support of the Brazilian Research Council (CNPq) and the Rio de Janeiro State Foundation of Research (FAPERJ).

References

Grebogi, C., Ott, E. and Yorke, J.A., 1983, "Crises, Sudden Changes in Chaotic Attractors, and Transient Chaos", *Physisca 7D*, pp.181-200.

Judge, J. and Pratap, R., 1998, "Asymptotic States of a Bilinear Hysteretic Oscillator in a Fully Dissipative Phase Space", *Journal of Sound and Vibration*, v.218(3), pp. 548-557.

Moon, F.C., 1992, "*Chaotic and Fractal Dynamics*", John Wiley.

Mullin, T., 1993, "*The Nature of Chaos*", Oxford Press.

Ortiz, M., Pinsky, P.M. and Taylor, R.L., 1983, "Operator Split Methods for the Numerical Solution of the Elastoplastic Dynamic Problem", *Computer Methods in Applied Mechanics and Engineering*, v.39, 137-157.

Poddar, B., Moon, F.C. and Mukherjee, S., 1988, "Chaotic Motion of an Elastic-Plastic Beam", *ASME Journal of Applied Mechanics*, v.55, pp.185-189.

Pratap, R., Mukherjee, S. and Moon, F.C., 1994, "Dynamic Behavior of a Bilinear Hysteretic Elasto-Plastic Oscillator, Part I: Free Oscillations", *Journal of Sound and Vibration*, v. 172(3), pp. 321-337.

Pratap, R., Mukherjee, S. and Moon, F.C., 1994, "Dynamic Behavior of a Bilinear Hysteretic Elasto-Plastic Oscillator, Part II: Oscillations Under Periodic Impulse Forcing", *Journal of Sound and Vibration*, v.172(3), pp. 339-358.

Pratap, R. and Holmes, P.J., 1995, "Chaos in a Mapping Describing Elastoplastic Oscillators", *Nonlinear Dynamics*, v.8, pp. 113-139.

Savi, M.A. and Pacheco, P.M.C.L., 1997, "Non-Linear Dynamics of an Elasto-Plastic Oscillator with Kinematic and Isotropic Hardening", *Journal of Sound and Vibration*, v.207(2), pp. 207-226.

Shanley, F.R., 1947, "Inelastic Column Theory", *Journal of the Aeronautical Sciences*, v.14, pp. 261-267.

Simo, J.C. and Taylor, R.L., 1985, "Consistent Tangent Operators for Rate-Independent Elastoplasticity", *Computer Methods in Applied Mechanics and Engineering*, v.48, pp. 101-118.

Symonds, P.S. and Yu, T.X., 1985, "Counterintuitive Behavior in a Problem of Elastic-Plastic Beam Dynamics", *ASME Journal of Applied Mechanics*, v.52, pp. 517-522.

Symonds, P.S., McNamara, J.F. and Genna, F., 1986, "Vibrations and Permanent Displacement of a Pinended Beam Deformed Plastically by Short Pulse Excitation", *International Journal of Impact Engineering*, v.4, pp. 73-82.